JOURNAL OF AIRCRAFT
Vol. 47, No. 5, September–October 2010

Engineering Notes

Yaw Control of a Tailless Aircraft Configuration

Gloria Stenfelt* and Ulf Ringertz†
Royal Institute of Technology, 100 44 Stockholm, Sweden

DOI: 10.2514/1.C031017

Introduction

MANY new aircraft configurations involve a tailless design with sweptback wings but without conventional fin and rudder. Recent examples of such designs are the B-2 and the X-45C demonstrator which are mainly optimized for low radar signature. The tailless sweptback wing planform was already introduced in the 1930s with the sailplane Ho 1 and the powered aircraft Ho 5, among many other designs by the Horten brothers [1]. In those days, the purpose of having an all-wing aircraft was reduced drag through a clean design and a not so complicated structural design, among other advantages presented by Nickel and Wohlfahrt [2]. In the United States, Jack Northrop continued with all-wing designs, e.g., the N-1M, which had split differential drag control surfaces near the wing tips for creating directional control [3].

However, in recent years, only the B-2 is in operational service [4] and there are few tailless aircraft under development. While these designs perform well during subsonic cruise missions, their ability as a fighter aircraft is under consideration. The handling qualities during fast maneuvers need to be improved and taken care of by a flight control system. Correct modeling with time delays and actuator models needs to be performed early in the design process [4].

The purpose of the present study is to investigate the control efficiency of the configuration shown in Fig. 1. Directional control is achieved using a split flap command to increase the drag on one wing to generate a yaw moment in the corresponding direction. Control laws are designed and implemented for testing in a wind tunnel at different airspeeds and angles of attack. Here, a model is used with two flaps located next to each other on the trailing edge of each wing. For creating drag, one flap is deflected up and the other down, hence, this is the definition of a split flap deflection in this study.

Model Description and Experimental Setup

A wind tunnel model has been designed and manufactured for low-speed wind tunnel testing. The model has previously been used in investigations of the steady-state aerodynamics [5]. The model can be mounted using a conventional sting exiting the tail pipe of the engine exhaust or on a fuselage mounted yaw sting through the top of the fuselage as shown in Fig. 1. The sting is mounted in the floor of the tunnel and the angle of attack can be adjusted by tilting the sting. Typical dimensions of the wind tunnel model are given in Table 1, and further details on this configuration are given in [5].

Using the yaw sting installation in the wind tunnel as shown in Fig. 1, the model can rotate freely in the yaw degree of freedom. Precision bearings in the yaw sting are used to minimize friction, but some effect of the friction can be observed in some testing because of the small aerodynamic forces involved. The yaw angle is measured with a potentiometer mounted inside the sting and a rate sensor is placed inside the model for measuring the yaw rate simultaneously. The yaw sting can also be modified to incorporate an internal torsional spring with variable stiffness. With the spring installed, the yaw sting arrangement is used for free oscillation testing making it possible to estimate yaw-damping derivatives.

The four trailing-edge control surfaces are actuated using electrical servos which are controlled using a custom designed Ethernet interface. A split flap deflection on one wing gives a yaw moment in the direction of the wing with deflected flaps. The split flap deflection is defined as positive if the outer flap goes up and the inner flap goes down. In this study, only positive deflections are used but the differences between using positive and negative split flap deflections are discussed in [5]. Measurements of the yaw moment due to sideslip and due to split flap deflections have been performed using a strain gauge balance for both sting configurations in order to estimate the sting interference effects.

Yaw Control Model

The lateral equation of motion for the yaw degree of freedom is given by

$$J\ddot{\psi} = N \tag{1}$$

where ψ is the yaw displacement and N the yaw moment following the notation of Etkin and Reid [6]. The mass moment of inertia J in Table 1 was obtained from a yaw ground vibration test using the yaw sting with a torsional spring installed.

Using standard notation, the sideslip angle is given by $\beta = -\psi$ and the yaw rate is $r = \dot{\psi}$. The aerodynamic forces can then be expressed in the form

$$N = -C_{n_\beta} qSb\psi + (C_{n_r} - C_{n_{\dot{\beta}}}) \frac{qSb^2}{2u} r \tag{2}$$

where q is the dynamic pressure and u the airspeed. The non-dimensional aerodynamic coefficients C_{n_β}, C_{n_r} and $C_{n_{\dot{\beta}}}$ represent the yaw moment produced by sideslip, yaw rate and a sideslip rate, respectively. Values for C_{n_β} at different freestream velocities and angles of attack, α, are retrieved experimentally from strain gauge balance measurements, while the combined coefficient $C_{n_r} - C_{n_{\dot{\beta}}}$ is found by evaluating vibration tests on the yaw sting with torsion spring.

Adding the influence of control caused by a split flap deflection δ_s gives an additional yaw moment C in Eq. (1) resulting in the equation of motion given by

$$J\ddot{\psi} = N + C(\delta_s) = N + \bar{C} + \Delta C \tag{3}$$

where

$$\bar{C} = C_{n_\beta} qSb\bar{\psi} \tag{4}$$

is the target yaw moment for the yaw angle $\bar{\psi}$ set point and

$$\Delta C = k_p(\psi - \bar{\psi}) + k_d r \tag{5}$$

is the deviation in the yaw moment from the target yaw moment. The controller is of standard proportional-derivative type with k_p and k_d representing proportional gain and derivative gain, respectively. Note

Received 11 November 2009; revision received 24 May 2010; accepted for publication 25 May 2010.

*Ph.D. Student, Division of Flight Dynamics; glorias@kth.se.
†Professor, Division of Flight Dynamics; rzu@kth.se.

Fig. 1 Yaw setup in the low-speed wind tunnel.

that for steady state, ($\dot{\psi} = \ddot{\psi} = 0$) and for a perfect case where $\psi = \bar{\psi}$, Eq. (3) is simply $N = -\bar{C}$.

An equation of motion for the closed-loop system can now be formed as

$$\begin{bmatrix} \dot{\psi} \\ \dot{r} \end{bmatrix} = \begin{bmatrix} 0 & 1 \\ -C_{n_\beta}\frac{qSb}{J} + \frac{k_p}{J} & (C_{n_r} - C_{n_{\dot{\beta}}})\frac{qSb}{J}\frac{b}{2u} + \frac{k_d}{J} \end{bmatrix} \begin{bmatrix} \psi \\ r \end{bmatrix} + \begin{bmatrix} 0 \\ C_{n_\beta}\frac{qSb}{J} - \frac{k_p}{J} \end{bmatrix} \bar{\psi} \tag{6}$$

This system can be identified as a time-dependent state space model linearized around the target sideslip angle $\bar{\psi} = -\bar{\beta}$ in the form

$$\dot{\mathbf{x}} = \mathbf{A}\mathbf{x} + \mathbf{B}\mathbf{c} \tag{7}$$

$$\mathbf{y} = \mathbf{C}\mathbf{x} \tag{8}$$

The output $\mathbf{y}$ is ψ or r and $\mathbf{C}$ is a scaling matrix converting radians to degrees. The system is now in a form suitable for analysis in standard software such as MATLAB.

However, for implementation in the wind tunnel, it is necessary to compute the actual split flap setting that gives the desired yaw moment. Unfortunately, the yaw moment is a nonlinear function of the split flap deflection requiring some special consideration. Here, a nonlinear model in the form

$$\delta_s = c_1\sqrt{|C(\delta_s)|} + c_2|C(\delta_s)| + c_3|C(\delta_s)|^2 \tag{9}$$

is used to compute the needed split flap deflection δ_s giving a desired yaw moment coefficient $C(\delta_s)$. The yaw moment coefficient measured for a large number of different split flap deflections are then used to find the parameters c_1, c_2 and c_3 using a least squares fit to the experimental data obtained in the previous study [5]. The first square root term in Eq. (9) may appear odd but is reasonable since the yaw moment is found to be well represented by a quadratic dependence on δ_s for small values of δ_s as discussed in [5]. The additional terms in the expression Eq. (9) improve the accuracy significantly at very little extra computational cost.

Table 1 Dimensions of the wind tunnel model

Entity	Notation	Value
Span	b	1.0 m
Mean chord	c	0.3373 m
Wing area	S	0.3373 m^2
Leading-edge sweep	Γ	56°
Trailing-edge flap chord	c_{TE}	0.04 m
Trailing-edge flap deflection interval	δ	±20°
Mass moment of inertia	J	0.2247 kgm^2
Test Reynolds number 1	Re_1	4.65×10^5
Test Reynolds number 2	Re_2	6.96×10^5

In the wind tunnel implementation of the control system, the control moment $C(\delta_s)$ is calculated using Eqs. (4) and (5) for given values of k_p, k_d and $\bar{\psi}$ and by measuring ψ and r in real time. The new flap deflection Eq. (9) is updated with a frequency of 20 Hz. The sign of $C(\delta_s)$ decides on which wing the flaps are deflected. For an unstable configuration and a positive $\bar{\beta}$, the nose goes to the left and the produced negative yaw moment N must be controlled with a counteracting positive yaw moment. Hence, a deflection on the right wing is needed. The data acquisition system and the control system for the wind tunnel model are implemented in LabVIEW.

Results

The aerodynamic derivatives used in the state space model were first measured with the yaw sting setup shown in Fig. 1 and the results were compared with those obtained with conventional tail mounted sting. For the static derivative, C_{n_β}, differences are very small and can be neglected. Recalling that static stability in yaw is defined as $C_{n_\beta} = \partial C_n/\partial\beta > 0$ [6], the wind tunnel model has been shown to be unstable at low angles of attack, while it is statically stable at high angles of attack [5].

Dynamic stability is investigated by performing vibration tests in yaw with the torsional spring installed. The state space model Eq. (7) is used without control and ($C_{n_r} - C_{n_{\dot{\beta}}}$) is tuned to match experimental results for different speeds. In the current configuration, the model is found to be unstable for all angles of attack.

In Table 2, values on the aerodynamic derivatives that are used in the following are listed. The freestream velocities $u = 20$ m/s and $u = 30$ m/s correspond to the test Reynolds numbers Re_1 and Re_2 given in Table 1, respectively. Although, the values for ($C_{n_r} - C_{n_{\dot{\beta}}}$) are of the same order of magnitude as the ones for C_{n_β}, a small change in these values does not influence the step response of the model significantly when compared with changing C_{n_β} with the same amount. For conventional aircraft a C_{n_β} value larger than 0.057 per radian is recommended to obtain satisfactory flying qualities [7]. Here, the value is negative and of one order of magnitude less for the low angles of attack. It is also said [7] that directional stability is found to be improved at higher angles of attack, which is found here as well.

For the yaw moment produced by a split flap deflection, the sting interference is significant. The yaw moment obtained for a given split flap deflection and using the two different sting arrangements in the wind tunnel are shown in Fig. 2. The yaw moment for a certain split flap deflection is lower having the sting mounted through the tail compared with the moment obtained using the yaw sting arrangement. Since it is important to use the correct c_1, c_2 and c_3 parameters when setting the flap deflection, Eq. (9), the new values for the yaw sting arrangement are used. Otherwise, the correct target sideslip angle would not be reached. In Fig. 2, it is also shown that the yaw moment due to a split flap deflection is close to be independent from the sideslip angle up to approximately 10 deg.

Step responses at zero angle of attack, constant gain setting and $u = 30$ m/s are shown for several target sideslip angles in Fig. 3. The best match between the model and the experimental results occurs for small $\bar{\beta}$. A steady-state test has shown, that the model can keep a maximum sideslip angle of 15 deg using the current gain setting.

Table 2 Derivatives obtained from experiments

Case/derivative	C_{n_β} (1/rad)	($C_{n_r} - C_{n_{\dot{\beta}}}$) (1/rad/s)
$u = 20$ m/s, $\alpha = 0$ deg	−0.00484	−0.0025
$u = 30$ m/s, $\alpha = 0$ deg	−0.00562	−0.0025
$u = 30$ m/s, $\alpha = 5$ deg	−0.00563	−0.0040
$u = 30$ m/s, $\alpha = 8$ deg	−0.01167	−0.0040
$u = 30$ m/s, $\alpha = 15$ deg	0.00978	0.0090

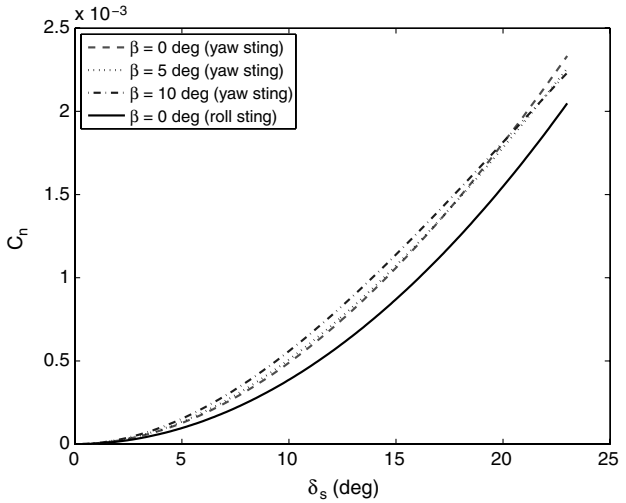

Fig. 2 Fit to experiments. Yaw moment vs split flap deflection for two sting setups at $u = 30$ m/s and $\alpha = 0$ deg.

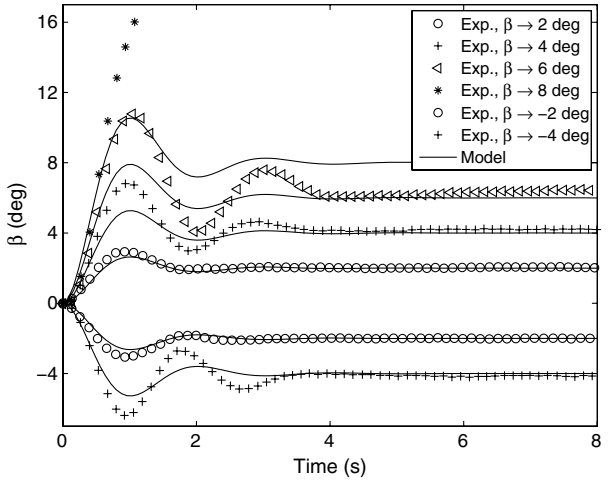

Fig. 3 Step response in β for $u = 30$ m/s and $\alpha = 0$ deg with $k_p = -3.5$ and $k_d = -0.5$.

Hence, the wind tunnel model departs already for $\bar{\beta} = 8$ deg, since the response overshoot exceeds 15 deg (see Fig. 3). To be able to take larger steps in β, it is required to increase the damping by increasing k_d. A drawback is then that the response becomes much slower.

The state space model is sufficient for estimating acceptable gain values by examining the eigenvalues of $\boldsymbol{A}$ in Eq. (7). For $\alpha = 0$, the model depends more on the direct influence of the freestream velocity on the dynamic pressure, than on the change of the values for the static and dynamic derivatives according to Table 2. In Fig. 4 it can be seen that with constant $k_p = -1$ and $k_d = -0.1$ the system is stable for $u = 20$ m/s, but for $u = 30$ m/s, the system is unstable and the wind tunnel model departs. In practice, the proportional gain is too small to achieve a sufficiently large split flap deflection and it is not possible to counteract the increased yaw moment due to the increase in aerodynamic forces. Hence, the absolute value on the gains need to be increased to establish a stable system, both for the simulation model and for the experiment.

For the lower airspeed of $u = 20$ m/s in Fig. 4, the experimental result shows higher damping in the response in comparison to the model prediction. The main reason for the difference appears to be stick slip friction in the experiment. At higher freestream velocities this effect is not as apparent. Since it has been shown that the model only fits the experiments for small target side slips, $\bar{\beta} = 4$ deg is chosen to be a compromise. The stick slip friction is too large for

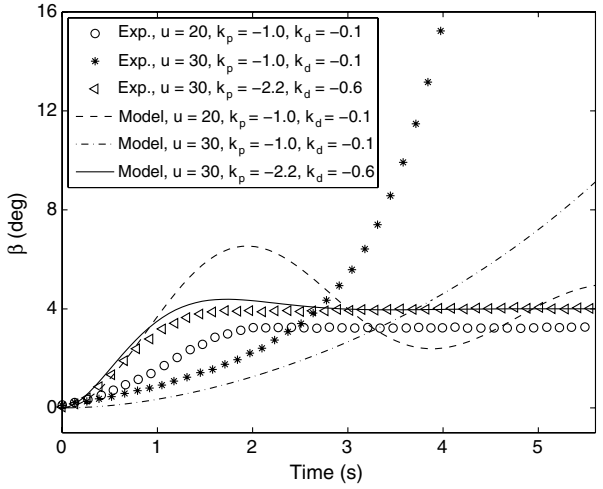

Fig. 4 Step response in β for different gains and speeds at $\alpha = 0$ deg.

smaller sideslips, and already here, it can be seen that the target position is not reached for the lower velocity.

Now, consider a constant freestream velocity of 30 m/s, and instead, the angle of attack is changed. In Fig. 5 the step response for the high angle of attack is less damped than for the lower angles of attack. The state space model almost coincides for $\alpha = 0$ and $\alpha = 5$ deg, mainly due to the fact that C_{n_β} and $(C_{n_r} - C_{n_{\dot{\beta}}})$ are very similar. However, the experiments differ showing a faster response for $\alpha = 5$ deg. From Fig. 5 the conclusion can be made that it is possible to find the robust values $k_p = -2.5$ and $k_d = -0.5$ that stabilize the model for both the lower angles and the higher angle of attack.

However, there are particular angles of attack where the dynamics of the closed-loop system requires thorough examination. A particularly interesting value is $\alpha = 8$ deg with the response shown in Fig. 6. This angle of attack has been identified by looking at large dips or peaks in the value on C_{n_β} with respect to different angles of attack. Using the same values $k_p = -2.5$ and $k_d = -0.5$ leads to an instability for the experiment and the proportional gain has to be decreased to at least -4.0 to reach stability. Also, the match between the model and the experiment is not satisfactory. Further, it has been noticed during the tests that the step responses are not repeatable at this angle of attack and this makes robust modeling difficult.

It is of interest to obtain the same step response for different α, however, as shown in Fig. 5, this can not be achieved with the same gain values. Assume that the optimal step response is given by the model response for $\alpha = 0$ and $\alpha = 5$ deg in the same figure. There, it takes about 2 s to reach the target sideslip angle and the overshoot is

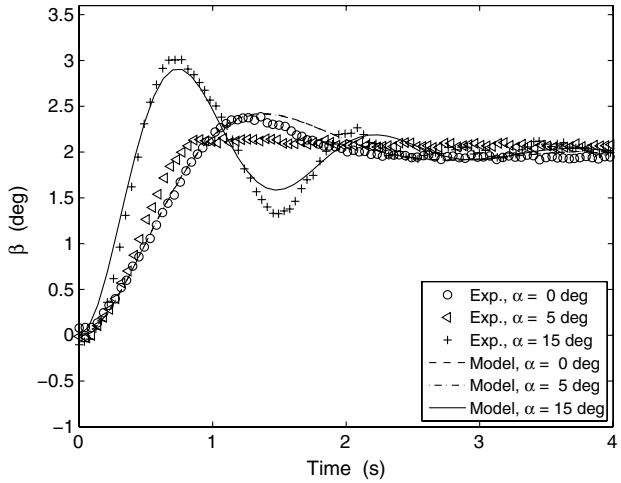

Fig. 5 Step response in β for $u = 30$ m/s and different angles of attack with $k_p = -2.5$ and $k_d = -0.5$.

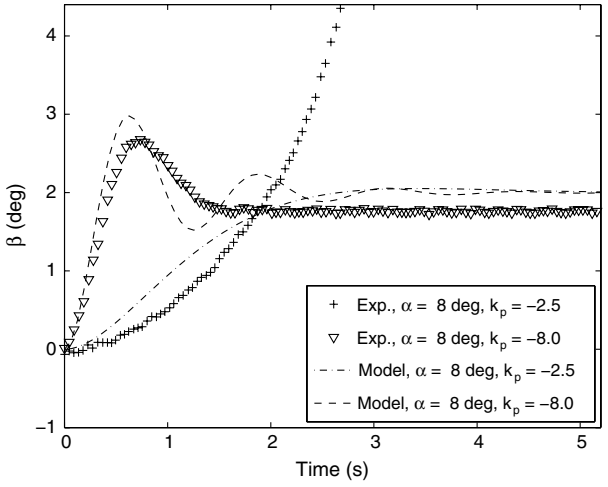

Fig. 6 Step response in β for $\alpha = 8$ deg with $k_d = -0.5$.

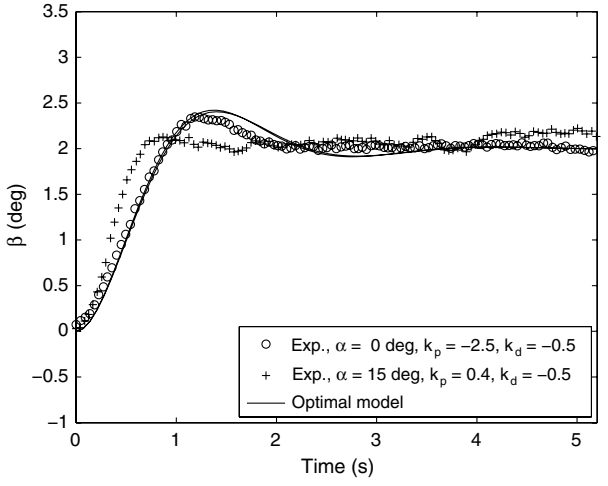

Fig. 7 Optimal gain values.

approximately 20%. To achieve the same step response with the state space model for $\alpha = 15$ deg the proportional gain needs to be increased to 0.4. Then, the models coincide and still fit well with the experiment at $\alpha = 0$, see Fig. 7. By contrast, the experiment shows a higher damping and quicker response for $\alpha = 15$ deg. The difference can have many reasons. A main part can be due to the drastic change in aircraft aerodynamics compared with the low angle of attack case. In a previous study [5] it has been shown by oil-flow visualization that a strong leading-edge vortex is present already at $\alpha = 11$ deg. This is reflected in the aerodynamic derivative C_{n_β} that has been obtained and used here as a constant for simplifying the state space model. In reality, C_{n_β} varies somewhat and is only a constant in even smaller β intervals. However, the simple state space model used here can give a hint on the experimental response and it is shown that both the experiments and the model depend strongly on C_{n_β}, which varies both with freestream velocity and with angle of attack. Hence, for some optimal step response, it is required to introduce gains that depend on both airspeed and angle of attack. For the full scale aircraft, compressibility is also an issue making it necessary to find suitable gains that are functions of at least three different parameters such as altitude, Mach number and angle of attack.

Conclusions

Designing efficient and robust control systems for flying wing configurations appears quite difficult as demonstrated in this paper. Apart from the lack of stability in yaw, the dynamics is also strongly dependent on the angle of attack. Gain scheduling may often be limited to only consider altitude and some form of airspeed such as the Mach number. Adding also the need for considering the angle of attack increases complexity significantly since it can change very quickly. Only modest changes in angle of attack gives significant changes in dynamics and the control system will need to consider this. Particularly difficult situations will be to design a good control system for landing in crosswind and gusts where both sideslip and angle of attack may change quickly. Simultaneously, the required control surface deflections can be large due to the low dynamic pressure when landing. The present configuration uses only four flaps for simultaneous control around all three axes and necessary control surface deflections for pitch, roll and yaw need to be superimposed at all times.

The conventional modeling approach with aerodynamics represented in the form of coefficient derivatives may not be sufficient either. Future investigations should focus on improved modeling making simulation more accurate. The lack of a conventional fin makes all forces small in the yaw degree of freedom and frictional forces make more important contributions both to steady-state and unsteady aerodynamic forces. However, the nonlinear dependence between the yaw moment and the split flap deflection appears to be straight-forward to treat using the approach presented in this paper.

Further research on the present configuration will be directed to high angle of attack and sideslip conditions. A particularly interesting case is the design of an automatic recovery procedure that can manage to restore a normal flight condition after departure.

Acknowledgments

This project is financially supported by the Swedish Defence Materiel Administration. The authors also wish to thank Marianne Jacobsen for her support when performing this study.

References

[1] Myhra, D., *The Horten Brothers and Their All-Wing Aircraft*, Schiffer Military/Aviation History, Schiffer, Lancaster, PA, 1998.

[2] Nickel, K., and Wohlfahrt, M., *Tailless Aircraft in Theory and Practice*, AIAA Education Series, AIAA, Reston, VA, 1998.

[3] Crenshaw, K., and Flanagan, B., "Testing the Flying Wing," AIAA Modeling and Simulation Technologies Conference and Exhibit, AIAA Paper 2002-4609, 2002.

[4] Colgren, R., and Loschke, R., "To Tail or Two Tails? The Effective Design and Modeling of Yaw Control Devices," AIAA/ASME/SAE/ASEE Joint Propulsion Conference and Exhibit, AIAA Paper 1997-3262, 1997.

[5] Stenfelt, G., and Ringertz, U., "Lateral Stability and Control of a Tailless Aircraft Configuration," *Journal of Aircraft*, Vol. 46, No. 6, 2009, pp. 2161–2164. doi:10.2514/1.41092

[6] Etkin, B., and Reid, L. D., *Dynamics of Flight, Stability and Control*, 3rd ed., Wiley, New York, 1996.

[7] Donlan, C. J., "An Interim Report on the Stability and Control of Tailless Airplanes," Langley Stability Research Center, TR 796, 1944.